Amino Acids (2006) 30: 477–493
DOI 10.1007/s00726-005-0281-y

Amino Acids
Printed in Austria

Aberrant expression of cytoskeleton proteins in hippocampus from patients with mesial temporal lobe epilepsy

J. W. Yang[1,*], **T. Czech**[2,*], **M. Felizardo**[1], **C. Baumgartner**[3], and **G. Lubec**[1]

[1] Department of Pediatrics, Medical University of Vienna, Vienna, Austria
[2] Department of Neurosurgery, Medical University of Vienna, Vienna, Austria
[3] Section of Clinical Epilepsy Research, Department of Neurology, Medical University of Vienna, Vienna, Austria

Received March 1, 2005
Accepted April 6, 2005
Published online April 4, 2006;

Summary. Mesial temporal lobe epilepsy (MTLE), the most common form of epilepsy, is characterised by cytoarchitectural abnormalities including neuronal cell loss and reactive gliosis in hippocampus. Determination of aberrant cytoskeleton protein expression by proteomics techniques may help to understand pathomechanism that is still elusive. We searched for differential expression of hippocampal proteins by an analytical method based on two-dimensional gel electrophoresis (2-DE) coupled with mass spectrometry unambiguously identifying 77 proteins analysed in eight control and eight MTLE hippocampi. Proteins were quantified and we observed 18 proteins that were altered in MTLE. Cytoskeleton proteins tubulin α-1 chain, β-tubulin, profilin II, neuronal tropomodulin were significantly reduced and one actin spot was missing, whereas ezrin and vinculin were significantly increased in MTLE. Proteins of several classes as e.g. antioxidant proteins (peroxiredoxins 3 and 6), chaperons (T-complex protein 1-α, stress-induced-phosphoprotein 1), signaling protein MAP kinase kinase 1, synaptosomal proteins (synaptotagmin I, α-synuclein), NAD-dependent deacetylase sirtuin-2 and 26S protease regulatory subunit 7 protein, neuronal-specific septin 3 were altered in MTLE. Taken together, the findings may represent or lead to cytoskeletal impairment; aberrant antioxidant proteins, chaperons, MAP kinase kinase 1 and NAD-dependent deacetylase sirtuin-2 may have been involved in pathogenetic mechanisms and altered synaptosomal protein expression possibly reflects synaptic impairment in MTLE.

Keywords: Antioxidant – Chaperone – Cytoskeleton – Hippocampus – Mesial temporal lobe epilepsy (MTLE)

Introduction

Mesial temporal lobe epilepsy (MTLE) represents the most common structural abnormality of human epilepsies and forms the pathological substrate of a syndrome associated with hippocampal sclerosis (Engel, 1996). It is now well established that epilepsy-induced morphological plasticity means sprouting of mossy fibers and cell death in CA1, CA3 and hilar cells associated with reactive gliosis in hippocampus, one of the most plastic brain regions. Although morphological features of MTLE are well known and have been studied in hippocampus of patients with MTLE and in many experimental models for epilepsy (Nadler, 2003; Shetty et al., 2003; Yamamoto et al., 1997), pathomechanism underlying structural changes is still elusive.

Several studies proposed the involvement of the cytoskeleton in neuropathology of MTLE. Increased α1-tubulin mRNA levels were reported in CA3 and dentate gyrus of hippocampus from the rat kindling model of epilepsy and suggested that microtubule formation is contributing to synaptic remodeling, such as mossy fiber sprouting and reorganization of neural networks of kindling-induced epileptogenicity (Sato and Abe, 2001). Hendriksen et al. (2001) showed increased gene expression levels of α-tubulin following status epilepticus in a kainic acid (KA) rat model using serial analysis of gene expression (SAGE). mRNA and immunoreactivity of α-tubulin were enhanced in granule cell bodies and in granule cell dendrites and axons (the mossy fibers) in a KA animal model (Represa et al., 1993). Pollard et al. (1994) reported that increased expression of α-tubulin protein was accompanied by overexpression of mRNA and microtubule-associated proteins MAP 2 and TAU-immunoreactivity in a comparable KA model. Zhu et al. (2000) isolated a highly expressed sequence, ERG14, that showed 69% identity to rat microtubule-associated protein in hippocampus of rats during the early epileptic state using

* J. W. Yang and T. Czech have equally contributed to the paper.

mRNA differential display and proposed a link to axonal growth and synaptogenesis. Status epilepticus-induced gene expression was also studied using cDNA array analysis (Lukasiuk et al., 2003). Aberrant expression of 87 genes in hippocampus and 208 genes in temporal lobe involved in neuronal plasticity, gliosis, organisation of the cytoskeleton or extracellular matrix, cell adhesion, signal transduction, regulation of cell cycle and metabolism were observed. This gene hunting method provided basic information on molecular changes at the nucleic acid level during epileptogenesis and epilepsy in animal model.

However, important studies at the nucleic levels are, there is a long and unpredictable way from RNA to protein and RNA expression may not reflect protein expression. We therefore decided to carry out protein hunting enabled by the advent of proteomic methods allowing protein profiling in hippocampus specimen from patients with MTLE and controls. We are aware of the limitations of the method (Fountoulakis, 2001) but using this approach a series of cytoskeleton elements (Gulesserian et al., 2002; Lubec et al., 2001; Weitzdoerfer et al., 2002) and proteins of several cascades and pathways known to be involved in neurodegeneration (Bernert et al., 2002; Engidawork et al., 2003; Engidawork and Lubec, 2003; Kim et al., 2002a, b; Krapfenbauer et al., 2003; Vlkolinsky et al., 2001) were analysed in our previous studies.

Materials and methods

Patients and controls

Approval for this study was obtained from the Institutional Board of the University of Vienna. Specimens were obtained at surgery from 11 patients (8 patients for 2-DE) with drug-resistant MTLE with typical imaging features (Jackson et al., 1993) and pathological confirmation of hippocampal sclerosis (Babb and Brown, 1987) who had unilateral selective amygdalohippocampectomy or anteromedial temporal lobe resection. The decision for surgery was based on convergent evidence of clinical and EEG recordings during prolonged video-EEG monitoring and high-resolution magnetic resonance imaging (MRI) indicating mesial temporal lobe seizure onset. Informed consent was obtained from patients providing specimens. Surgical specimens were examined by routine pathology. As control tissue, 8 normal hippocampal samples were obtained at autopsy from patients (postmortem delay: max. 11 h) with no history of brain disease. Clinical information on MTLE patients and patients used as controls is presented in Table 1. Demonstration of clinical variables between MTLE group and control group is given in Table 2.

Table 1. Clinical characterisation of MTLE patients and controls

ID	Sex	Age (yrs)	Duration of epilepsy (yrs)	Side	Antiepileptic drugs (AED)
Patient with MTLE					
E1	F	42.7	36	L	CBZ, SVP, DPH, TIA
E2	M	39.9	15	R	LAM, CBZ, SVP
E3	F	38.0	34	R	OX, LEV, PB, TOP, LAM, PRIM, CBZ, VIG, SVP
E4	M	34.4	14	R	CBZ
E5	M	35.2	32	R	OX, PRIM, SVP
E6	F	21.5	13	L	SVP, TOP
E7	F	35.7	14	R	CBZ, TOP
E8	M	32.4	16	R	LEV, CBZ, TOP, LAM, SVP
E9	M	49.9	29	R	CBZ, SVP, TOP, LAM, PRIM
E10	M	44.0	19	L	TOP, VIG, LEV
E11	M	43.8	23	L	CBZ, TOP
ID	Sex	Age (yrs)	Post-mortem interval (hrs)	Side	Causes of death
Control					
C1	M	62.6	11	L	Coronary heart disease
C2	F	60.1	10	L	Cholangiocarcinoma
C3	M	56.4	10	R	Squamous cell carcinoma (retropharyngeal)
C4	M	73.1	6	L	Papillary renal cell carcinoma
C5	M	55.0	11	R	Squamous cell carcinoma (palate)
C6	M	44.2	11	R	Cardiormyopathy
C7	M	50.9	8	R	Pulmonary embolism
C8	M	53.7	8	L	Pneumonia

CBZ Carbamazepine; *DPH* Phenytoin; *LAM* Lamotrigine; *LEV* Levetiracetam; *OX* Oxcarbazepine; *PB* Phenobarbital; *PRIM* Primidone; *SVP* Sodium Valproate; *TIA* Tiagabine; *TOP* Topiramate; *VIG* Vigabatrin; *R* Right; *L* Left

Table 2. Comparison of clinical variables between MTLE group and control group

	2-DE		Western blot	
	Control	MTLE	Control	MTLE
Male:Female	7:1	5:3	4:1	4:4
Age (yrs) ± SD	57.0 ± 8.6	38.2 ± 8.9	61.4 ± 7.2	35.0 ± 6.4
Duration of epilepsy (yrs)	–	22.8 ± 8.7	–	21.8 ± 10.2
Post-mortem interval (hrs)	9.4 ± 1.8	–	9.6 ± 2.1	–
Side (Right:Left)	4:4	4:4	2:3	6:2
ID number (Table 1)	C1–C8	E1, E5–E11	C1–C5	E1–E8

Preparation of hippocampal specimens

Specimens were taken from the hippocampal body (middle segment): A tissue block of 5- to 10-mm thickness, perpendicular to the hippocampal axis was rapidly dissected on ice in order to remove any cortical tissue medial to subiculum as well as white matter from the parahippocampal gyrus. Hippocampi were immediately taken and stored into liquid nitrogen and the freezing chain was never interrupted until analysis.

Two-dimensional gel electrophoresis

Hippocampal tissue was ground in liquid nitrogen and suspended in 1 ml of sample buffer consisting of 7 M urea, 2 M thiourea, 4% CHAPS, 10 mM DTT, 1 mM EDTA, 1 mM PMSF and a mixture of protease inhibitors (Roche Diagnostics, Mannheim, Germany). After sonication for approximately 15 sec, the suspension was left at room temperature for 1 h and centrifuged at 14,000 × *g* for 60 min at 12 °C. Desalting was done with Ultrafree-4 centrifugal filter unit (Millipore, Bedford, MA, USA). The protein content of the supernatant was determined by the Coomassie blue method. 2-DE was performed essentially as reported with individual hippocampi (Yang et al., 2004). Samples of 1 mg protein were applied on immobilized pI 3–10 nonlinear gradient strips. Focusing started at 200 V and the voltage was gradually increased to 8,000 V at 4 V/min and kept constant for a further 3 h (approximately 150,000 Vh in total). The second-dimensional separation was performed on 9–16% gradient SDS polyacrylamide gels. The gels (180 × 200 × 1.5 mm) were run at 40 mA per gel. After protein fixation for 12 h in 50% methanol and 10% acetic acid, gels were stained with colloidal Coomassie blue (Novex, San Diego, CA, USA) for 8 h. Molecular masses were determined by running standard protein markers (Bio-Rad Laboratories, Hercules, CA, USA) covering the range 10–250 kDa. pI values were used as given by the supplier of the immobilized pH gradient strips (Amersham Bioscience, Uppsala, Sweden). Excess of dye was washed out from the gels with distilled water and the gels were scanned with ImageScanner (Amersham Bioscience). Image analysis and quantification of spots were performed with version 3.1 of ImageMaster 2D Elite software (Amersham Bioscience).

MALDI-TOF and MALDI-TOF/TOF – mass spectrometry (MS)

Spots were excised with a spot picker (PROTEINEER sp™, Bruker Daltonics, Leipzig, Germany), placed into 96-well microtiter plates and in-gel digestion and sample preparation for MALDI analysis were performed by an automated procedure (PROTEINEER dp™, Bruker Daltonics) (Suckau et al., 2003). Briefly, spots were excised and washed with 10 mM ammonium bicarbonate and 50% acetonitrile in 10 mM ammonium bicarbonate. After washing, gel plugs were shrunk by addition of acetonitrile and dried by blowing out the liquid through the pierced well bottom. The dried gel pieces were reswollen with 40 ng/µl trypsin (Roche Diagnostics) in enzyme buffer (consisting of 5 mM Octyl β-D-glucopyranoside (OGP) and 10 mM ammonium bicarbonate) and incubated for 4 h at 30 °C. Peptide extraction was performed with 10 µl of 1% TFA in 5 mM OGP. Extracted peptides were directly applied onto a target (AnchorChip™, Bruker Daltonics) that was loaded with α-cyano-4-hydroxycinnamic acid (Sigma, St. Louis, MO, USA) matrix thinlayer. The mass spectrometer used in this work was an Ultraflex™ TOF/TOF (Bruker Daltonics) operated in the reflector for MALDI-TOF peptide mass fingerprint (PMF) or LIFT mode for MALDI-TOF/TOF with a fully automated mode using the FlexControl™ software. An accelerating voltage of 25 kV was used for PMF. Calibration of the instrument was performed externally with $[M+H]^+$ ions of angiotensin I, angiotensin II, substance P, bombesin, and adrenocorticotropic hormones (clip 1–17 and clip 18–39). Each spectrum was produced by accumulating data from 200 consecutive laser shots and spectra were interpreted with the aid of the Mascot Software (Matrix Science Ltd, London, UK). For protein search, a mass tolerance of 100 ppm and 2 missing cleavage sites were allowed and oxidation of methionine residues was considered. The probability score calculated by the software was used as criterion for correct identification. Those samples which could not be identified by their PMF from MALDI-TOF were additionally analyzed using LIFT-TOF/TOF MS/MS from the same target. A maximum of three precursor ions per sample were chosen for MS/MS analysis. In the TOF1 stage, all ions were accelerated to 8 kV under conditions promoting metastable fragmentation. After selection of jointly migrating parent and fragment ions in a timed ion gate, ions were lifted by 19 kV to high potential energy in the LIFT cell. After further acceleration of the fragment ions in the second ion source, their masses could be analysed simultaneously in the reflector with high sensitivity. LIFT spectra were interpreted with the Mascot software. MS/MS tolerance of 0.5 Da and 1 missing cleavage sites were allowed and oxidation of methionine residues was considered. The probability score calculated by the software was used as criterion for correct identification. Finally, database searches, through Mascot, using combined PMF and MS/MS datasets were performed via BioTools 2.2 software (Bruker Daltonics).

Western blot analysis

Hippocampal tissue aliquots were homogenised in lysis buffer consisting of 10 mM Tris-HCl (pH 7.5), 150 mM NaCl, 0.05% Tween 20, 1% SDS and protease inhibitor cocktail, and centrifuged at 12,000 × *g* for 10 min at 4 °C. The protein concentration of the supernatant was measured with a BCA protein assay kit (Pierce, Rockford, IL, USA) using a standard curve constructed from BSA standards. After mixing samples with sample buffer (60 mM Tris-HCl, 2% SDS, 0.1% bromphenol blue, 25% glycerol, and 14.4 mM 2-mercaptoethanol, pH 6.8) and incubation at 95 °C for 5 min, samples were separated by 12.5% homogenous ExcelGel SDS gels (Amersham Bioscience) and electrotransferred onto PVDF membranes (MilliPore). After incubation in blocking solution (10 mM Tris-HCl, pH 7.5, 150 mM NaCl, 0.05% Tween 20 and 5% non-fat dry milk), membranes were incubated with synaptophysin (SYN) antibody (Sigma), neuronal specific enolase (NSE) antibody (NeoMarker, Fremont, CA, USA), actin antibody (Sigma) and glial fibrillar acidic protein (GFAP) antibody (Chemicon, Temecula, CA, USA) for 2 h at room temperature. After washing three times for 10 min with washing solution (0.3% Tween 20 in TBS), membranes were incubated with a horseradish peroxidase conjugated anti-mouse IgG_1 for synpatophysin, NSE and GFAP and anti-mouse IgG_2a for actin (Southern Biotechnology, Birmingham, AL, USA) for 1 hr at room temperature. Membranes were washed three times for 10 min and antigen–antibody complexes were visualized by an ECL reagent (Western Lightning™, PerkinElmer Life Sciences, Boston, MA, USA) on an X-ray film according to the manufacturer's protocol. Densities

of immunoreactive signaling bands were measured by RELPscan version 2.1 software program (Scanalytics, Billerica, MA, USA).

Statistical analysis

Data obtained from 2-DE quantification and immunoblotting are presented as mean ± standard deviation (SD). The statistical analysis was performed by the use of unpaired Student's t-test, Pearson correlation and Spearman correlation analysis using GraphPad InStat (version 3.06; San Diego, CA, USA) software and statistical significance was considered at the $P < 0.05$ level.

Results

Identification and quantification of proteins in human hippocampus

2-DE was performed with individual hippocampi (8 controls and 8 MTLEs) and gels were run in duplicate. Human hippocampal proteins were solubilized in the IEF-compatible lysis buffer including urea, thiourea and

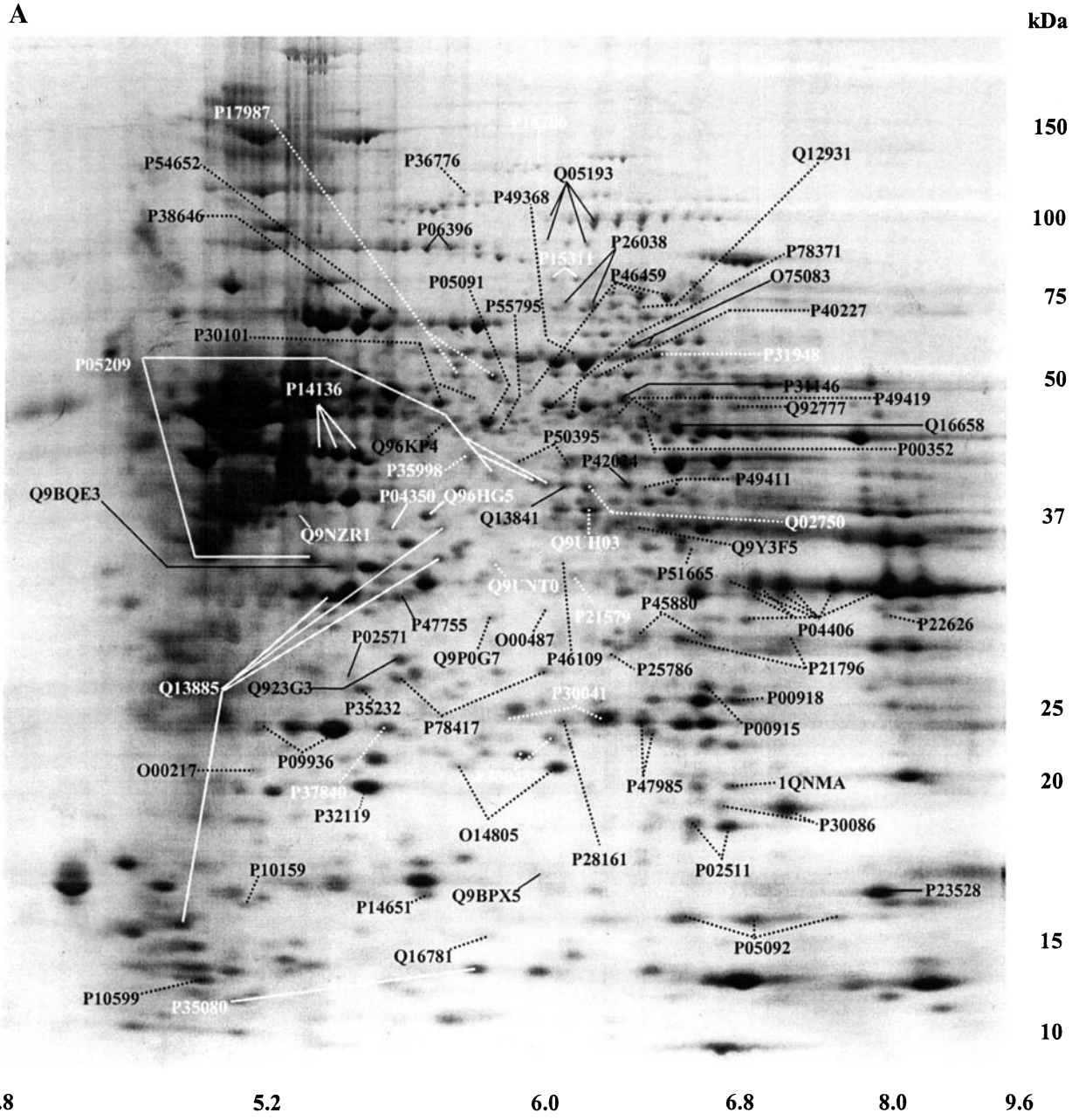

Fig. 1. The composite 2-DE maps of the human hippocampus from control (**A**) and MTLE patients (**B**). 2-DE was performed in an immobilised pI 3–10 nonlinear gradient strip, followed by second-dimensional separation on 9–16% gradient polyacrylamide gels and separated proteins were detected by colloidal Coomassie blue staining. Spots were analysed by MALDI TOF or TOF/TOF. Identified proteins (dot line), cytoskeleton proteins (solid line) and altered proteins (white) in MTLE are designated by their SWISS-PROT or NCBI accession number (Table 3). The names of proteins are listed in Table 3

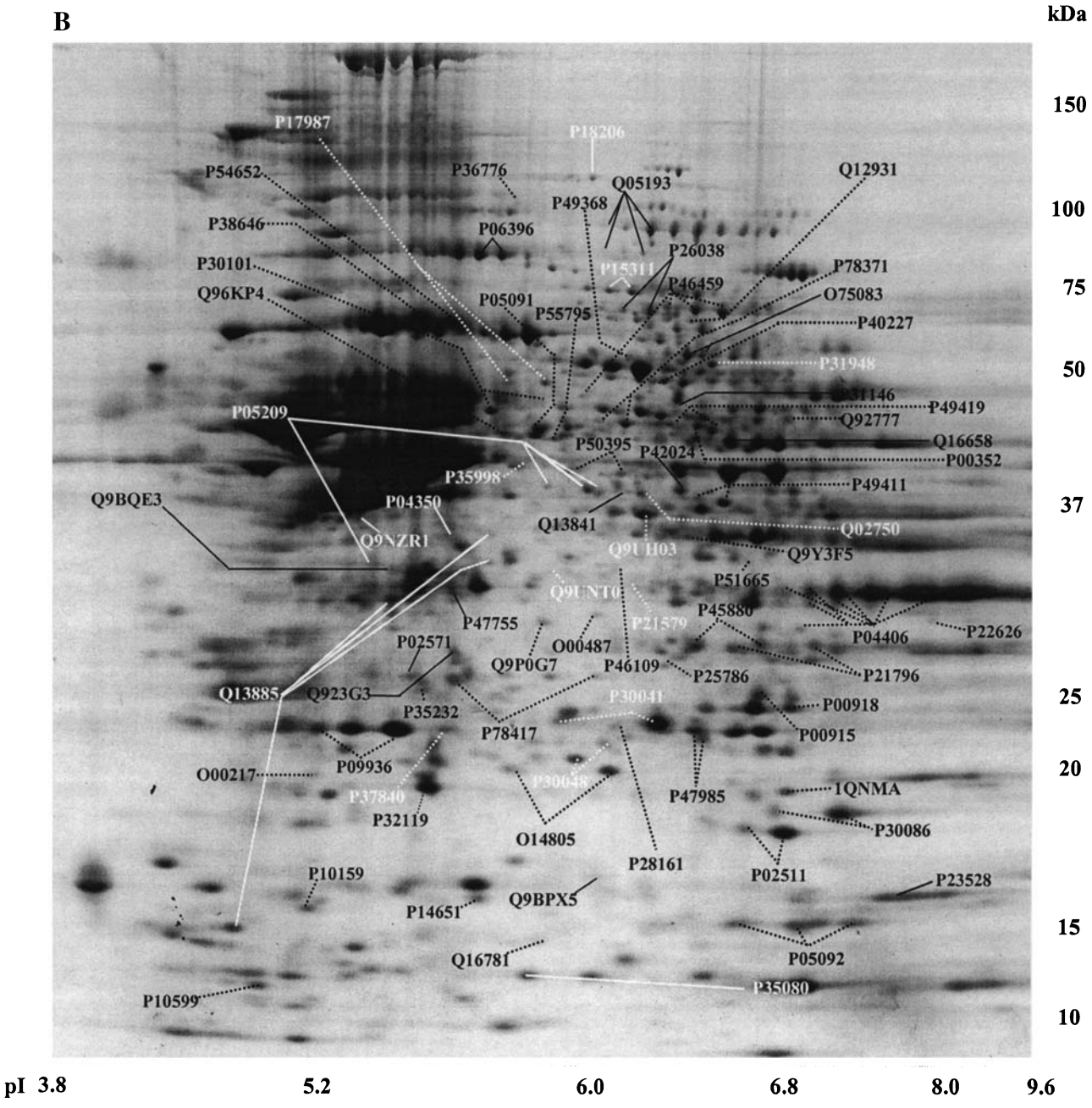

Fig. 1 (*continued*)

CHAPS, separated on broad pH range IPG strips (pI 3–10) and SDS-PAGE. A Coomassie blue stained representative gels containing identified and quantified proteins, constructed from control and MTLE hippocampus are shown in Fig. 1. A large series of spots were excised from 2-DE gels and after in-gel digestion, 121 spots corresponding to 77 different proteins were unambiguously identified using MALDI-TOF or TOF/TOF and Mascot database searching. Protein spots were outlined (first automatically and then manually) and relative intensities were calculated as percentage of spot volume compared to total proteins on the gel (Fig. 1 and Table 3). Differently expressed proteins in hippocampus of MTLE are given in Fig. 2 and Table 3.

Expression profile of proteins in hippocampus

Figure 2 shows differently expressed proteins in MTLE with partial 2-DE images and Table 3 includes protein names and synonyms of 12 proteins with decreased and

Table 3. Identification and quantification of proteins in human hippocampus

No.[a]	Protein name (Synonym)	Theoretical[b]		Observed		Matches	Score[c]	Control	MTLE
		pI	MW (Da)	pI	MW (kDa)				
	Cytoskeleton proteins								
O75083	WD-repeat protein 1 (Actin interacting protein 1)	6.17	66193.52	6.2	62	16	164	0.0756 ± 0.0341 (n = 8)	0.0814 ± 0.0465 (n = 8)
				6.3	62	14	113	0.0326 ± 0.0200 (n = 8)	0.0344 ± 0.0068 (n = 7)
P63261	Actin, cytoplasmic 2 (Gamma-actin)	5.31	41792.84	5.6	25	12	94	0.0296 ± 0.0072 (n = 8)	0.0276 ± 0.0128 (n = 8)
P04350	Tubulin beta-5 chain	4.81	49630.87	5.62	37	14	85	**0.0224 ± 0.0115** (n = 7)	**0.0390 ± 0.0089*** (n = 6)
P05209	Tubulin alpha-1 chain (Alpha-tubulin 1)	4.94	50151.63	5.4	36	11	134	**0.1545 ± 0.0746** (n = 8)	**0.0450 ± 0.0120**** (n = 8)
				5.86	38	14	141	0.0258 ± 0.0100 (n = 8)	0.0169 ± 0.0089 (n = 8)
				5.95	38	12	85	0.0414 ± 0.0175 (n = 7)	0.0559 ± 0.0238 (n = 8)
				6.0	38	14	121	**0.0630 ± 0.0230** (n = 8)	**0.0211 ± 0.0116***** (n = 7)
P06396	Gelsolin [precursor] (Actin-depolymerizing factor)	5.90	85697.52	5.7	90	8	67	0.1596 ± 0.0739 (n = 8)	0.2439 ± 0.0847 (n = 8)
				5.75	90	10	81	0.1155 ± 0.0541 (n = 8)	0.1488 ± 0.0628 (n = 8)
P14136	Glial fibrillary acidic protein, astrocyte (GFAP)	5.42	49880.21	5.4	39	13	101	–	–
				5.45	39	7	88	–	–
				5.5	39	10	95	–	–
P15311	Ezrin (p81) (cytovillin) (villin 2)	5.95	69267.59	5.98	80	10	82	**0.0186 ± 0.0054** (n = 8)	**0.0625 ± 0.0272***** (n = 8)
				6.2	80	18	132	**0.0524 ± 0.0250** (n = 8)	**0.1856 ± 0.0394***** (n = 8)
P18206	Vinculin (Metavinculin)	5.51	123668.11	6.0	130	9	65	**0.0293 ± 0.0081** (n = 8)	**0.0451 ± 0.0081**** (n = 8)
P23528	Cofilin, non-muscle isoform	8.22	18502.49	7.9	16	11	174	0.5414 ± 0.1400 (n = 8)	0.4511 ± 0.2011 (n = 7)
P26038	Moesin (Membrane-organizing extension spike protein)	6.09	67688.85	6.05	75	10	67	0.0273 ± 0.0122 (n = 8)	0.0259 ± 0.0109 (n = 8)
				6.1	75	13	92	0.0577 ± 0.0277 (n = 7)	0.0519 ± 0.0371 (n = 8)
P31146	Coronin-1A (Coronin-like protein p57)	6.25	51026.25	6.2	46	11	118	0.0987 ± 0.0389 (n = 8)	0.0825 ± 0.0246 (n = 8)
P35080	Profilin II	6.78	14915.04	5.85	13	6	78	**0.4390 ± 0.0849** (n = 8)	**0.2784 ± 0.0628***** (n = 8)
P61163	Alpha-centractin (Centractin) (ARP1)	6.19	42613.74	6.2	38	19	154	0.0774 ± 0.0187 (n = 8)	0.0756 ± 0.0195 (n = 8)
P47755	F-actin capping protein alpha-2 subunit	5.58	32817.92	5.68	35	7	66	0.1311 ± 0.0294 (n = 8)	0.0846 ± 0.0563 (n = 8)
Q05193	Dynamin-1	6.93	97407.27	6.0	115	13	64	0.0070 ± 0.0045 (n = 7)	0.0134 ± 0.0070 (n = 8)
				6.12	115	27	194	0.0950 ± 0.0675 (n = 8)	0.1268 ± 0.0673 (n = 8)
				6.0	95	14	92	0.0118 ± 0.0047 (n = 8)	0.0081 ± 0.0015 (n = 7)
				6.1	95	14	88	0.0181 ± 0.0096 (n = 8)	0.0154 ± 0.0087 (n = 7)

(*continued*)

Table 3 (*continued*)

No.[a]	Protein name (Synonym)	Theoretical[b]		Observed		Matches	Score[c]	Control	MTLE
		pI	MW (Da)	pI	MW (kDa)				
Q13841	Beta-centractin [Fragment]	6.19	37096.63	6.05	37.8	15	117	0.0614 ± 0.0417 (n = 8)	0.0561 ± 0.0173 (n = 8)
Q13885	Beta tubulin (Tubulin, beta 2)	4.78	49906.97	4.95	15	13	111	0.1735 ± 0.0611 (n = 8)	0.2028 ± 0.0562 (n = 8)
				5.46	35	21	164	**0.3261 ± 0.1878** (n = 8)	**0.1711 ± 0.0444*** (n = 8)
				5.83	36.3	22	168	**0.0858 ± 0.0470** (n = 8)	**0.0200 ± 0.0099**** (n = 8)
				5.84	37	25	196	**0.0470 ± 0.0313** (n = 7)	**0.0104 ± 0.0078**** (n = 8)
Q16658	Fascin (Singed-like protein) (p55) (55 kDa actin bundling protein)	6.81	54398.81	6.35	40	7	73	0.1606 ± 0.0868 (n = 8)	0.2419 ± 0.3109 (n = 8)
Q923G3	Capping protein (Actin filament) muscle Z-line, beta	5.69	30628.74	5.65	27	11	70	0.1634 ± 0.0218 (n = 7)	0.1213 ± 0.0515 (n = 8)
Q96HG5	Actin, beta [Fragment]	5.56	41004.96	5.73	37	14	103	**0.1636 ± 0.0426** (n = 8)	**0.0 ± 0.0***** (n = 8)
Q9BPX5	Actin related protein 2/3 complex, subunit 5-like	6.15	16941.19	6.0	17	7	83	0.0538 ± 0.0181 (n = 8)	0.0411 ± 0.0126 (n = 8)
Q9BQE3	Tubulin alpha-6 chain	4.96	49895.33	5.45	36.3	11	80	0.1281 ± 0.0785 (n = 8)	0.0790 ± 0.0336 (n = 8)
Q9NZR1	Tropomodulin-2 (N-Tmod) (Neuronal tropomodulin)	5.21	39595.05	5.35	37	16	89	**0.0456 ± 0.0185** (n = 8)	**0.0268 ± 0.0153*** (n = 8)
	Antioxidant								
1QNMA[d]	Manganese superoxide dismutase (EC 1.15.1.1) mutant Q143N, chain A-Human	6.86	22190.1	6.7	20	7	68	0.2316 ± 0.1191 (n = 8)	0.1803 ± 0.0571 (n = 8)
O00217	NADH-ubiquinone oxidoreductase 23 kDa subunit, mitochondrial [Precursor]	6.00	23705.09	5.2	20	9	81	0.0411 ± 0.0205 (n = 7)	0.0236 ± 0.0124 (n = 8)
P00352	Retinal dehydrogenase 1 (Aldehyde dehydrogenase, cytosolic)	6.29	54730.65	6.22	42	15	118	0.0490 ± 0.0175 (n = 7)	0.0397 ± 0.0186 (n = 6)
P05091	Aldehyde dehydrogenase, mitochondrial [Precursor]	6.63	56381.32	5.88	40	23	196	0.2897 ± 0.0522 (n = 7)	0.2215 ± 0.0898 (n = 8)
P10599	Thioredoxin	4.82	11606.30	5.0	12	11	120	0.1285 ± 0.0518 (n = 8)	0.1144 ± 0.0511 (n = 8)
P28161	Glutathione S-transferase Mu 2	6.02	25613.46	6.05	24	10	107	0.0429 ± 0.0221 (n = 8)	0.0311 ± 0.0157 (n = 8)
P30041	Peroxiredoxin 6 (Antioxidant protein 2)	6.02	24903.79	5.9	24	11	98	**0.0319 ± 0.0151** (n = 7)	**0.0786 ± 0.0339**** (n = 7)
				6.0	24	13	130	0.5649 ± 0.1482 (n = 8)	0.6489 ± 0.3398 (n = 8)
P30048	Thioredoxin-dependent peroxide reductase, mitochondrial [Precursor] (Peroxiredoxin 3) (Antioxidant protein 1)	7.68	27692.65	5.95	22	12	148	**0.3659 ± 0.1007** (n = 8)	**0.2299 ± 0.0751**** (n = 8)
				6.01	23	9	87	**0.1128 ± 0.0305** (n = 8)	**0.0700 ± 0.0245*** (n = 8)
P32119	Peroxiredoxin 2 (Thioredoxin peroxidase 1)	5.66	21891.92	5.55	20	7	91	0.8988 ± 0.1645 (n = 8)	0.7595 ± 0.1310 (n = 8)

(*continued*)

Table 3 (*continued*)

No.[a]	Protein name (Synonym)	Theoretical[b]		Observed		Matches	Score[c]	Control	MTLE
		pI	MW (Da)	pI	MW (kDa)				
P47985	Ubiquinol-cytochrome C reductase iron-sulfur subunit, mitochondrial [Precursor]	8.55	29651.99	6.24	24	10	78	0.1770 ± 0.0300 (n = 8)	0.1585 ± 0.0622 (n = 8)
				6.25	23	9	80	0.1460 ± 0.0823 (n = 8)	0.0819 ± 0.0301 (n = 8)
P49419	Aldehyde dehydrogenase family 7 member A1	6.24	55235.18	6.18	41	14	156	0.0427 ± 0.0116 (n = 6)	0.0414 ± 0.0228 (n = 7)
				6.28	41	17	117	0.0575 ± 0.0309 (n = 6)	0.0597 ± 0.0237 (n = 7)
P78417	Glutathione transferase omega 1	6.24	27565.86	5.64	28	9	67	0.1284 ± 0.0429 (n = 8)	0.0863 ± 0.0786 (n = 8)
				6.0	28.5	7	64	0.1229 ± 0.0414 (n = 7)	0.0376 ± 0.0258 (n = 8)
	Chaperones								
P02511	Alpha crystallin B chain	6.76	20158.91	6.45	18	10	116	0.1760 ± 0.0499 (n = 8)	0.1260 ± 0.0509 (n = 8)
				6.7	18	8	76	0.5580 ± 0.1788 (n = 8)	0.6860 ± 0.1743 (n = 8)
P62937	Peptidyl-prolyl cis-trans isomerase A	7.82	17881.30	6.35	16	9	103	0.2483 ± 0.0694 (n = 7)	0.2678 ± 0.0644 (n = 8)
				6.9	16	7	71	0.3486 ± 0.1313 (n = 7)	0.3854 ± 0.2213 (n = 8)
				7.7	16	9	113	0.2269 ± 0.1320 (n = 7)	0.1649 ± 0.1408 (n = 8)
P17987	T-complex protein 1, alpha subunit (TCP-1-alpha)	5.80	60343.58	5.8	51	12	68	0.0395 ± 0.0225 (n = 8)	0.0239 ± 0.0096 (n = 8)
				5.88	50	20	184	**0.1295 ± 0.0348** (n = 8)	**0.0704 ± 0.0213**** (n = 8)
P30101	Protein disulfide isomerase A3 [Precursor] (Disulfide isomerase ER-60) (ERp60) (p58)	5.98	56782.39	5.76	44	24	190	0.1618 ± 0.0638 (n = 8)	0.1151 ± 0.0711 (n = 8)
				5.84	44.5	22	205	0.0254 ± 0.0158 (n = 8)	0.0130 ± 0.0110 (n = 7)
P31948	Stress-induced-phosphoprotein 1 (STI1) (Hsp70/Hsp90-organizing protein)	6.40	62639.26	6.25	58	18	108	**0.1269 ± 0.0544** (n = 8)	**0.0695 ± 0.0202*** (n = 8)
P35232	Prohibitin	5.57	29804.10	5.54	26	12	136	0.1417 ± 0.0609 (n = 8)	0.0908 ± 0.0386 (n = 8)
P38646	Stress-70 protein, mitochondrial [Precursor]	5.87	73680.50	5.53	70	25	256	0.2480 ± 0.1085 (n = 8)	0.1808 ± 0.0974 (n = 8)
P40227	T-complex protein 1, zeta subunit (TCP-1-zeta)	6.24	58024.17	6.16	60	16	129	0.0255 ± 0.0120 (n = 8)	0.0156 ± 0.0064 (n = 8)
				6.20	60	17	152	0.1021 ± 0.0381 (n = 8)	0.0794 ± 0.0244 (n = 8)
P49368	T-complex protein 1, gamma subunit (TCP-1-gamma)	6.10	60402.69	6.08	55	20	168	0.0629 ± 0.0227 (n = 8)	0.0637 ± 0.0386 (n = 7)
P54652	Heat shock-related 70 kDa protein 2 (Heat shock 70 kDa protein 2)	5.56	70020.97	5.62	70	12	107	0.0583 ± 0.0191 (n = 8)	0.0337 ± 0.0253 (n = 6)
P78371	T-complex protein 1, beta subunit (TCP-1-beta) (CCT-beta)	6.01	57488.21	5.98	42	38	344	0.0210 ± 0.0108 (n = 6)	0.0145 ± 0.0043 (n = 8)
				6.08	42	22	162	0.1513 ± 0.0425 (n = 8)	0.1798 ± 0.0425 (n = 8)

(*continued*)

Table 3 (*continued*)

No.[a]	Protein name (Synonym)	Theoretical[b]		Observed		Matches	Score[c]	Control	MTLE
		pI	MW (Da)	pI	MW (kDa)				
Q12931	Heat shock protein 75 kDa, mitochondrial [Precursor]	8.05	80010.86	6.24	75	11	75	0.0247 ± 0.0105 (n = 7)	0.0183 ± 0.0070 (n = 7)
Q9P0G7	Lambda-crystallin	5.68	33358.78	5.88	35	10	68	0.0630 ± 0.0151 (n = 8)	0.0716 ± 0.0154 (n = 8)
	Proteolysis								
O00487	26S proteasome non-ATPase regulatory subunit 14	6.06	34577.04	6.0	35	14	85	0.0217 ± 0.0129 (n = 7)	0.0263 ± 0.0093 (n = 7)
P09936	Ubiquitin carboxyl-terminal hydrolase isozyme L1 (Neuron cytoplasmic protein 9.5)	5.33	24824.34	5.2	24	12	117	0.1253 ± 0.0747 (n = 8)	0.2069 ± 0.1305 (n = 8)
				5.45	24	15	121	1.3654 ± 0.5849 (n = 8)	1.1205 ± 0.5442 (n = 8)
P25786	Proteasome subunit alpha type 1	6.15	29555.59	6.16	30	10	63	0.0531 ± 0.0198 (n = 8)	0.0435 ± 0.0166 (n = 8)
P35998	26S protease regulatory subunit 7 (MSS1 protein)	5.72	48502.66	5.82	38.8	10	62	**0.0263 ± 0.0094** (n = 8)	**0.0489 ± 0.0146**** (n = 8)
P36776	Lon protease homolog, mitochondrial [Precursor] (Lon protease-like protein) (LONP)	6.01	106489.30	5.81	120	12	79	0.0140 ± 0.0072 (n = 8)	0.0100 ± 0.0047 (n = 8)
P51665	26S proteasome non-ATPase regulatory subunit 7	6.29	37025.40	6.39	36.5	8	66	0.0225 ± 0.0094 (n = 6)	0.0161 ± 0.0088 (n = 7)
P61088	Ubiquitin-conjugating enzyme E2 N	6.13	17137.82	5.87	14.6	7	93	0.0804 ± 0.0262 (n = 8)	0.0551 ± 0.0235 (n = 8)
Q96KP4	Cytosolic nonspecific dipeptidase (Glutamate carboxypeptidase-like protein 1)	5.66	52878.47	5.77	40	15	91	0.0294 ± 0.0138 (n = 8)	0.0333 ± 0.0315 (n = 8)
	Signaling proteins								
P21796	Voltage-dependent anion-selective channel protein 1 (VDAC-1)	8.63	30641.40	6.34	32	11	82	0.1174 ± 0.0418 (n = 8)	0.1550 ± 0.0403 (n = 8)
				7.3	32	12	120	0.1565 ± 0.0939 (n = 8)	0.0901 ± 0.0415 (n = 7)
P30086	Phosphatidylethanolamine-binding protein (Neuropolypeptide h3)	7.43	20925.59	6.6	19	8	91	0.0760 ± 0.0337 (n = 8)	0.0849 ± 0.0293 (n = 8)
				7.3	19	13	160	0.8180 ± 0.2701 (n = 8)	0.8758 ± 0.4062 (n = 8)
P45880	Voltage-dependent anion-selective channel protein 2 (VDAC-2)	6.32	38092.73	6.23	33	8	82	0.3541 ± 0.6679 (n = 8)	0.1675 ± 0.0665 (n = 8)
				6.4	33	12	127	0.0944 ± 0.0558 (n = 8)	0.0669 ± 0.0329 (n = 8)
P50395	Rab GDP dissociation inhibitor beta (Rab GDI beta) (GDI-2)	6.11	50663.25	5.92	38.5	13	103	0.0381 ± 0.0196 (n = 8)	0.0290 ± 0.0165 (n = 8)
				6.05	38.5	32	288	0.0584 ± 0.0265 (n = 8)	0.04104 ± 0.0212 (n = 8)
Q02750	Dual specificity mitogen-activated protein kinase kinase 1 (MAP kinase kinase 1) (MAPKK 1) (MAPK/ERK kinase 1)	6.20	43307.82	6.12	37.5	18	114	**0.0805 ± 0.0293** (n = 8)	**0.0283 ± 0.0148***** (n = 7)
Q9Y3F5	A6 related protein (Twinfilin-like protein)	6.37	39548.04	6.22	36.8	13	124	0.0280 ± 0.0145 (n = 6)	0.0250 ± 0.0139 (n = 7)

(*continued*)

Table 3 (*continued*)

No.[a]	Protein name (Synonym)	Theoretical[b]		Observed		Matches	Score[c]	Control	MTLE
		pI	MW (Da)	pI	MW (kDa)				
	Synaptosomal, neuronal and brain proteins								
P00915	Carbonic anhydrase I	6.63	28739.02	6.45	27	14	164	0.1504 ± 0.0895 (n = 8)	0.1890 ± 0.0733 (n = 8)
P00918	Carbonic anhydrase II	6.86	29114.86	6.7	26	11	116	0.2670 ± 0.1144 (n = 8)	0.2288 ± 0.0797 (n = 8)
P21579	Synaptotagmin I (SytI) (p65)	8.26	47573.11	6.08	36	17	114	**0.0973 ± 0.0503** (n = 7)	**0.0116 ± 0.0062***** (n = 7)
P37840	Alpha-synuclein (Non-A beta component of AD amyloid)	4.67	14460.16	5.6	24	4	71	**0.1626 ± 0.0406** (n = 8)	**0.0888 ± 0.0321**** (n = 8)
P46459	Vesicle-fusing ATPase (Vesicular-fusion protein NSF)	6.38	82654.36	5.97	47	13	68	0.0183 ± 0.0096 (n = 6)	0.0169 ± 0.0058 (n = 7)
				6.16	76	11	67	0.0235 ± 0.0081 (n = 8)	0.0210 ± 0.0115 (n = 6)
				6.22	76	14	125	0.0775 ± 0.0405 (n = 8)	0.0670 ± 0.0426 (n = 7)
				6.29	76	10	89	0.1466 ± 0.0683 (n = 8)	0.1333 ± 0.0655 (n = 7)
Q92777	Synapsin II	8.57	62968.37	6.7	45	13	94	0.0299 ± 0.0131 (n = 8)	0.0446 ± 0.0639 (n = 8)
Q9UH03	Neuronal-specific septin-3	6.74	39345.38	6.12	37	8	61	**0.1790 ± 0.0521** (n = 8)	**0.2625 ± 0.0710*** (n = 8)
	Transcriptional proteins								
Q99497	DJ-1 protein (Oncogene DJ1)	6.33	19891.05	5.82	22	9	104	0.1486 ± 0.0853 (n = 8)	0.1099 ± 0.0410 (n = 8)
				6.04	22	9	96	0.5031 ± 0.0499 (n = 8)	0.4039 ± 0.1320 (n = 8)
P63241	Eukaryotic translation initiation factor 5A (eIF-5A) (eIF-4D)	5.08	16701.06	5.15	16	6	72	0.0633 ± 0.0406 (n = 7)	0.0681 ± 0.0496 (n = 8)
P14651	Homeobox protein Hox-B3	9.27	44344.21	5.72	16.5	4	62	0.1960 ± 0.0750 (n = 8)	0.1523 ± 0.0573 (n = 8)
P46109	Crk-like protein	6.26	33776.99	6.04	36.3	7	66	0.0202 ± 0.0170 (n = 6)	0.0126 ± 0.0048 (n = 8)
P49411	Elongation factor Tu, mitochondrial [Precursor]	7.26	49541.54	6.25	37.6	21	235	0.0309 ± 0.0161 (n = 8)	0.0176 ± 0.0065 (n = 7)
				6.32	37.6	22	185	0.1075 ± 0.0463 (n = 8)	0.1062 ± 0.0468 (n = 8)
P55795	Heterogeneous nuclear ribonucleoprotein H′ (hnRNP H′)	5.89	49263.57	5.89	39.6	16	145	0.0418 ± 0.0249 (n = 8)	0.0384 ± 0.0252 (n = 8)
Q8IXJ6	NAD-dependent deacetylase sirtuin-2 (SIR2-like) (SIR2-like protein 2)	5.22	43182.17	5.87	36.2	18	182	**0.0316 ± 0.0135** (n = 8)	**0.0056 ± 0.0085***** (n = 7)
	Housekeeping protein								
P04406	Glyceraldehyde 3-phosphate dehydrogenase, liver (EC 1.2.1.12) (GAPDH)	8.58	35922.02	6.68	35.8	12	67	0.0873 ± 0.0373 (n = 8)	0.1195 ± 0.0860 (n = 8)
				7.0	35.8	16	119	0.1951 ± 0.0636 (n = 8)	0.2541 ± 0.1671* (n = 8)
				7.2	35.8	18	131	0.4019 ± 0.1329 (n = 8)	0.4620 ± 0.1809 (n = 8)

(*continued*)

Table 3 (*continued*)

No.[a]	Protein name (Synonym)	Theoretical[b]		Observed		Matches	Score[c]	Control	MTLE
		pI	MW (Da)	pI	MW (kDa)				
				7.7	35.8	18	129	**0.5414 ± 0.1658** (n = 8)	**0.3754 ± 0.1323*** (n = 8)
				8.3	35.8	13	91	1.0221 ± 0.3169 (n = 8)	0.8158 ± 0.3310 (n = 8)
				6.9	35.5	15	134	0.0673 ± 0.0540 (n = 6)	0.0540 ± 0.0324 (n = 8)
				7.2	35.5	12	116	0.0950 ± 0.0322 (n = 6)	0.0725 ± 0.0321 (n = 8)
				6.8	34	14	129	0.0393 ± 0.0209 (n = 6)	0.0248 ± 0.0086 (n = 6)

Proteins from the hippocampus were extracted and separated by 2-DE as described in Materials and methods. The proteins were identified by MALDI TOF or TOF/TOF, following in-gel digestion with trypsin. The search in protein databases was performed with MASCOT software. The score calculated by the software and more than 61 scores and at least four matched peptides (Matches) were used as criterion for correct identification. Protein spots were outlined (first automatically and then manually) and quantified using the ImageMaster 2D Elite software. The percentage of the volume of spots representing a certain protein was determined in comparison with the total proteins present in the whole gel. Values are expressed as mean ± standard deviation of percentage of the spot volume. The statistical analysis was evaluated by unpaired Student's t-test and statistical significance was considered at $^{*}P<0.05$, $^{**}P<0.01$ and $^{***}P<0.001$

[a] Accession number of SWISS-PROT (http://www.expasy.org/sprot/)

[b] Calculated for the corresponding SWISS-PROT entry using the ExPASy Compute pI/MW tool in ExPASy website (http://www.expasy.org)

[c] Score is -10^{*}Log (P), where P is the probability that the observed match is a random event (MASCOT, http://www.matrixscience.com/help/scoring-help.html)

[d] Accession number of NCBI database (http://www.ncbi.nlm.nih.gov)

6 proteins with increased levels in MTLE printed in bold.

The major components of microtubules, tubulin alpha-1 chain (P05209), beta tubulin (Q13885) and tubulin beta-5 chain (P04350) were identified and 2 of 4 spots of tubulin alpha-1 chain and 3 of 4 spots of beta tubulin were significantly decreased in MTLE ($P<0.05$) while tubulin beta-5 chain was significantly increased ($P<0.05$). Among actin-related proteins, capping protein ezrin (P15311) and actin-anchoring protein vinculin (P18206) were significantly increased ($P<0.01$) and profilin II (P35080) and neuronal tropomodulin (Q9NZR1) were decreased ($P<0.05$) in MTLE. The fragmented form of beta-actin (Q96HG5) was missing in MTLE.

In the antioxidant protein group, one of 2 spots that were identified as peroxiredoxin 6 (P30041) was comparable, the other was increased significantly in MTLE ($P<0.01$) and another member of the peroxiredoxin family, peroxiredoxin 3 (syn.: thioredoxin-dependent peroxide reductase; P30048) was decreased ($P<0.05$). One spot of T-complex protein 1 alpha (P17987, 2 spots), chaperone protein, and stress-induced phosphoprotein 1 (P31948) was decreased significantly ($P<0.05$) in MTLE.

Further differences observed were increase of 26S protease regulatory subunit 7 (P35998) and neuronal-specific septin 3 (Q9UH03) and decreased expression levels of dual specificity mitogen-activated protein kinase 1 (Q02750), synaptotagmin I (P21579), alpha-synuclein (P37840) and NAD-dependent deacetylase sirtuin-2 (Q8IXJ6) in MTLE as compared to controls.

Expression of marker proteins in control and MTLE

To consider cytoarchitectural abnormalities in MTLE versus housekeepings and so-called marker proteins, we performed Western blotting with antibodies against GFAP, NSE, SYN and actin, widely used as reference proteins, although not unequivocally accepted (Fig. 3A). Glyceraldehyde 3-phosphate dehydrogenase (GAPDH) was selected as reference protein for representing total cell number from 2-DE. Although 1 out of 8 spots was altered in MTLE (Table 3), the sum of 8 GAPDH spots in each 2-DE gel was comparable between controls (2.3990 ± 0.3571) and MTLE (2.1719 ± 0.4492) as shown in Fig. 3B. Total cell density was estimated by comparable expressions of housekeeping protein actin on Western blot and the sum of GAPDH spots on 2D gels between controls and MTLE and no difference was observed. Expression of NSE, widely considered as a marker for neuronal density (Marangos and Schmechel, 1987) and synapto-

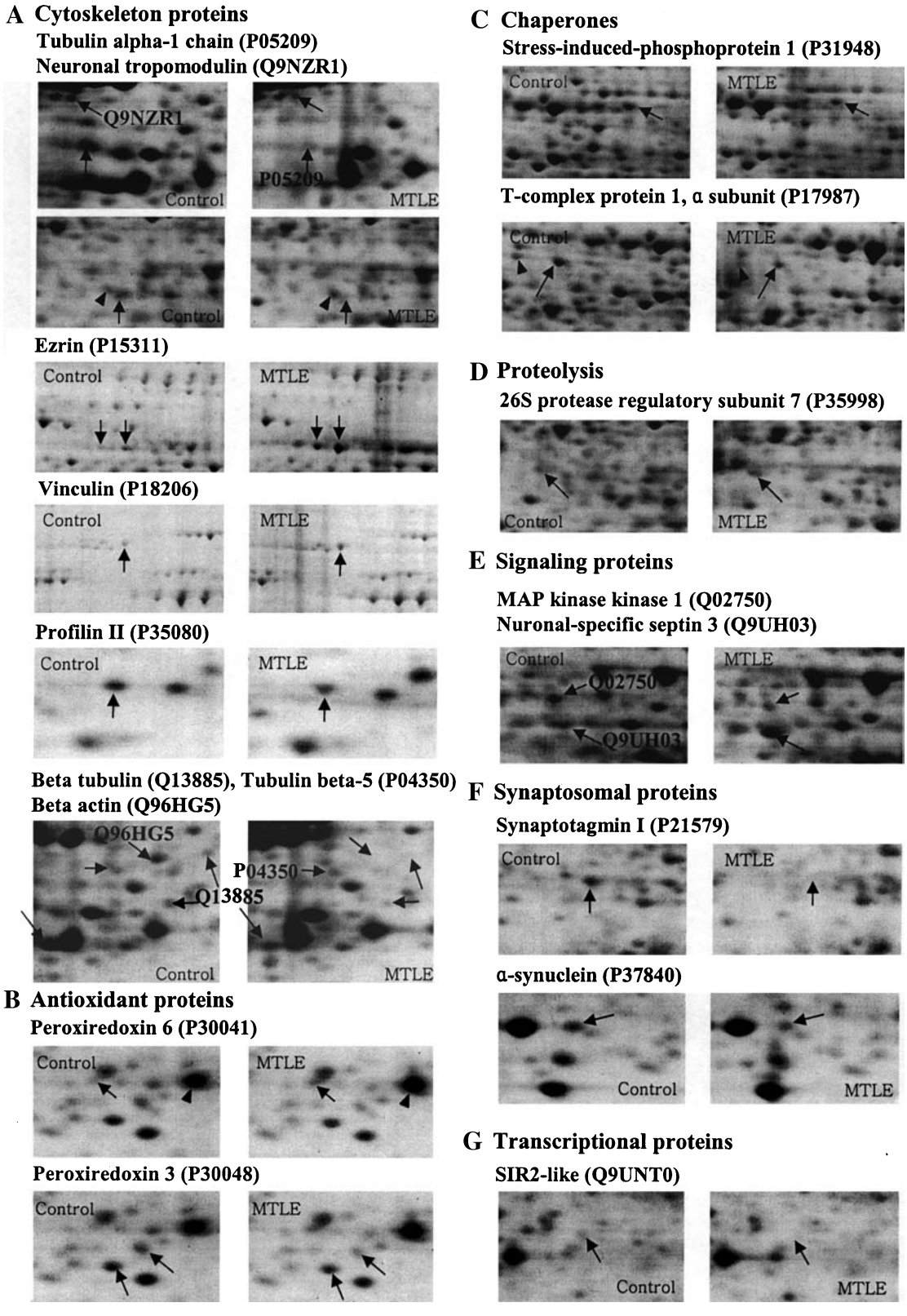

Fig. 2A–G. Partial 2-DE images demonstrating alterations of protein expression in MTLE. The area of interest was cut out of the whole gel image for proteins that were differently expressed in hippocampus from MTLE compare to control. Names of proteins are given on top of the figure and arrows show the corresponding spots with significant difference and arrowheads show the corresponding spots that are comparable between two groups

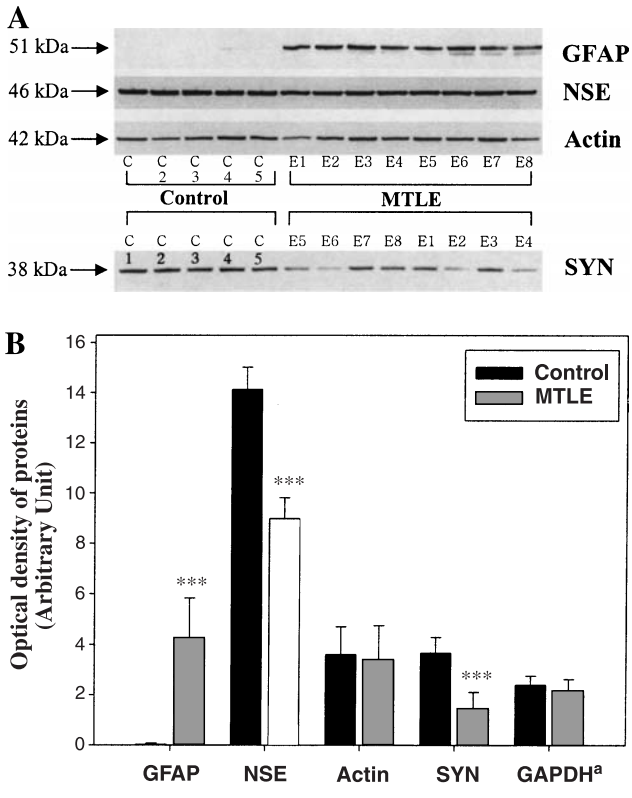

Fig. 3. Western blot patterns of GFAP, NSE, actin and synaptopysin (SYN) in hippocampi from controls and patients with MTLE (**A**). Denatured proteins for GFAP (1 μg/lane), NSE (5 μg/lane), actin (5 μg/lane) and SYN (5 μg/lane) were separated on 12.5% homogeneous gels and transferred onto PVDF membranes and subsequently reacted with antibodies against GFAP (1:4000), NSE (1:750), actin (1:2000) and SYN (1:3000), respectively. The expression levels of proteins were expressed as the mean ± SD of optical density of immunoreactive bands (**B**). In comparison with controls, the level of significance was considered at $^{*}P < 0.05$ and $^{***}P < 0.001$. [a]Data are from the sum of GAPDH spots expression on each 2-DE gel (Table 3)

physin, a marker for synaptic reinnervation, synaptic density and synaptogenesis (Lopez et al., 2003), were significantly decreased in MTLE (Fig. 3B). Immunoreactive GFAP, proposed to be representing cell density of astroglial lineage (Reeves et al., 1989), was highly increased in MTLE possibly representing gliosis. Increased GFAP was also observed on 2-DE gels of MTLE hippocampi (data not shown): highly increased GFAP spots were overlapping, however, on 2-DE gels of MTLE specimen making quantification of each individual spot impossible.

Discussion

The major finding of this study is aberrant expression of several cytoskeleton proteins represented by decreased or increased expressional levels. The fact that some structures showed expression comparable to controls or were even showing higher levels shows the specificity of results and that changes are not simply due to reduced cell density, which in turn has been shown to be comparable between controls and MTLE revealed by comparable housekeeping proteins, actin and GAPDH. Differences between expression of several spots representing the same protein, probably reflecting splicing forms or posttranslational modifications, may explain aberrant expression of some cytoskeleton proteins. The stoichiometry of cytoskeleton elements, essential for structural integrity (Pollak et al., 2003) was herein shown to be seriously impaired and was mainly affecting the microtubular system although ezrin, vinculin, and profilin II – linking actin based cytoskeleton elements to the plasma membrane – were affected as well.

The cytoskeleton is a highly dynamic structure not only forming the scaffold, the basis of cell morphology and plasticity but plays a major role in transport and signaling (Brady et al., 2003). It is comprised of three major types of cytoplasmic structural proteins: microtubules, actin and intermediate filaments. Microtubules, are mainly composed of heterodimers of α and β tubulin, perform essential and diverse functions in eukaryotic cells including chromosome segregation – mitosis and meiosis and determine cellular morphology and size, axonal transport, neuronal polarity (Baas, 2002), mortality, and organelle distribution (Dutcher, 2001; Hadfield et al., 2003). The actin cytoskeleton is a complex structure serving the control of cellular shape, distribution of membrane proteins, intracellular trafficking mechanisms (Eitzen, 2003) as well as generation and motility of growth cones, spines and dendrites (Brown and Bridgman, 2004; Brady et al., 2003; dos Remedios et al., 2003; Engidawork and Lubec, 2003). Derangement of the brain's cytoskeleton including several structures shown above has been reported in different forms of neurodegenerative disease including Down Syndrome and Alzheimer's disease (AD) and may reflect or lead to neuropathological changes as e.g. neuronal death and synaptosomal loss (Gulesserian et al., 2002; Lubec et al., 2001; Shim and Lubec, 2002; Weitzdoerfer et al., 2002).

The decrease of several tubulin α and β spots observed herein is in disagreement with previous studies that reported increased gene or immunoreactivity level of alpha-tubulin in experimental epilepsy models (see above). Divergent results may be explained by methodological differences as well as discrepancies between gene and protein levels. Recently, we found 63 and 19 tubulin spots (alpha and beta forms) in primary rat neurons and astro-

cytes, repectively (Yang et al., 2005) and this different expression pattern may help to explain the decrease of several tubulin spots in MTLE based on neuronal loss which is a well known feature of MTLE. The decrease of neuronal tropomodulin, a conserved family of actin-capping proteins, may not only represent neuronal cell loss in MTLE but also affect cytoskeleton integrity in MTLE. Sussman et al. (1994) reported an increase of neuronal tropomodulin mRNA and moderate elevation of protein levels in the dentate gyrus of the hippocampus following prolonged seizure activity induced by kainic acid.

We identified three isoforms of peroxiredoxin, increased peroxiredoxin 6, decreased peroxiredoxin 3 and comparable peroxiredoxin 2 in MTLE. Peroxiredoxin 6 can be distinguished from peroxiredoxin 2 and 3 with its unique one-cysteine structure and is localised in mitochondria and peroxisomes while peroxiredoxin 3 exists in mitochondria only (Fujii and Ikeda, 2002; Wang et al., 2003). Wang et al. (2003) generated peroxiredoxin 6-targeted mutant mice and reported that lack of peroxiredoxin 6 led to high levels of hydrogen peroxide, significantly lower survival rates, severe tissue damage and higher protein oxidation level. They demonstrated that function of peroxiredoxin 6 was independent of other peroxiredoxins including peroxiredoxin 3 and other antioxidant proteins. This may help to explain different peroxiredoxin patterns in MTLE. Increased peroxiredoxin 6 (syn.: antioxidant protein 2) in MTLE is in agreement with previous proteomics result in brain of KA-treated rats inducing status epilepticus (Krapfenbauer et al., 2001). Alteration of high abundance brain antioxidant proteins peroxiredoxin 6 and peroxiredoxin 3 may propose a role of oxidative stress for development of cytoskeleton impairment. Increased peroxiredoxin 6 may be reactively overexpressed following reactive oxygen attack and decreased peroxiredoxin 3 may have been even allowing the generation of reactive oxygen species. Both antioxidant enzymes have been shown to be linked to neurodegenerative processes as shown previously (Krapfenbauer et al., 2002, 2003) and oxidative stress in brain of patients with temporal lobe epilepsy has been documented using *in vivo* (1)H-MR spectroscopy (Mueller et al., 2001).

Involvement of chaperons in the process of neurodegenerative disorders (Yoo et al., 2001a, b) including epilepsies has been previously reported (Yenari, 2002). The chaperons whose levels were changed in our observation are major candidates for chaperoning cytoskeleton elements: in particular T-complex protein 1 structures are specific for tubulin (Schuller et al., 2001). Impairment of chaperons may well have been responsible for development of the cytoskeletal deficit but may as well reflect a byphenomenon only, as status epilepticus per se is followed by overexpression of several heat shock components (Little et al., 1996), although different from the elements TCP-1-alpha and STI1, observed in this study.

An about three-fold decrease of dual specificity mitogen-activated protein kinase kinase 1 (MAPKK1) was observed and this may contribute to cytoskeletal alteration by impaired phosphorylation of cytoskeleton proteins, proteins known to be substrates of MAP kinase kinases (Horne and Guadagno, 2003). MAPKK also shows a link to synaptic function (Hoeffer et al., 2003) and the observed decrease of MAPKK1 in this report may partly help to explain the synaptosomal deficit in MTLE, herein represented by manifold decreased synaptotagmin I (Syt I) and alpha-synuclein. Syt I, a known exocytotic protein, is widely accepted as the primary calcium sensor for synaptic vesicle exocytosis. Recently, Poskanzer et al. (2003) suggested a function of Syt I during *in vivo* synaptic vesicle endocytosis by inactivating Syt I only during endocytosis. The observed decrease of Syt I in MTLE is consistent with the depression of Syt I mRNA in CA1 and CA3 hippocampal fields from adult rat brains following KA induced seizures (Tocco et al., 1996).

Alpha-synuclein, localised at the presynaptic region of axons, regulating dopamine release and transport and forming filamentous aggregates that are the non-amyloid components of synucleinopathies including Parkinson's disease, has never been reported to be associated with any form of epilepsy before. Therefore reduction of this structure that induces fibrillogenesis of microtubular-associated proteins may be involved in the synaptic deficit as well as in cytoskeletal abnormalities.

Neuronal-specific septin 3 in MTLE, a novel member of the septin subfamily of GTPase enzymes and required for the cytokinesis stage of cell division and exocytosis, was significantly increased. Although there are no reports linking this protein to epilepsies, aberrant expression of the polymorphic septin 3 alleles in AD supported a role for the pathogenesis of neurodegeneration (Takehashi et al., 2004).

The about 5.6-fold decrease of NAD-dependent deacetylase sirtuin-2 (SIR2-like), a NAD-dependent deacetylase colocalising with microtubules, that has never been associated with any human epilepsy as well, is a key element of transcriptional silencing, DNA repair and controlling cellular life span (Dryden et al., 2003). Decreased levels maybe explaining multiple expressional differences observed in MTLE as e.g. neuronal death and probably

Table 4. Relationships of protein spot expression level to age in control group

ID[a]	Protein name	n[b]	Pearson		Spearman	
			r[c]	P	r[c]	P
P05209	Tubulin alpha-1 chain	8	−0.6344	0.0912	−0.5000	0.2162
Q13885	Beta tubulin	8	−0.1190	0.7930	−0.0155	0.9710
		8	0.3981	0.3287	0.2619	0.5364
		7	0.0957	0.8382	0.1071	0.8397
P04350	Tubulin beta-5 chain	7	0.1144	0.8071	0.2143	0.6615
		8	−0.4093	0.3140	−0.3810	0.3599
P15311	Ezrin	8	−0.2745	0.5105	−0.0238	0.9768
		8	−0.4369	0.2791	−0.5714	0.1511
P18206	Vinculin	8	0.0423	0.9208	−0.0714	0.8820
P35080	Profilin II	8	−0.1252	0.7677	−0.1905	0.6646
Q96HG5	Actin, beta [Fragment]	8	0.5356	0.1713	0.7143	0.0576
Q9NZR1	Neuronal tropomodulin	8	−0.1112	0.7932	−0.0952	0.8401
P30041	Peroxiredoxin 6	7	0.6501	0.1139	0.6071	0.1667
P30048	Peroxiredoxin 3	8	0.3440	0.4040	0.1190	0.7930
P17987	T-complex protein 1, alpha subunit	8	0.2661	0.5241	0.5000	0.2162
P31948	Stress-induced-phosphoprotein 1	8	−0.6329	0.0921	−0.7143	0.0576
P35998	26S protease regulatory subunit 7	8	0.3286	0.4267	0.0952	0.8401
Q02750	Dual specificity mitogen-activated protein kinase kinase 1	8	−0.2656	0.5249	6.608E-19	>0.9999
P21579	Synaptotagmin I	7	−0.2693	0.5592	−0.2857	0.5560
P37840	Alpha-synuclein	8	0.2124	0.6136	0.4524	0.2675
Q9UH03	Neuronal-specific septin 3	8	0.5185	0.1880	0.5238	0.1966
Q8IXJ6	NAD-dependent deacetylase sirtuin-2	8	−0.1539	0.7160	−0.1667	0.7033

[a] Accession number of SWISS-PROT (http://www.expasy.org/sprot/)
[b] Sample number
[c] Correlation coefficient (r)

decreased DNA repair. Deficient SIR2-like in MTLE furthermore fits or maybe even generating cytoskeletal deterioration as this protein is known to specifically deacetylate tubulin (North et al., 2003). Knockout of this protein leads to tubulin hyperacetylation and one may speculate that this posttranslational modification leads to structural and functional changes and probably to quantitative alterations. It is intriguing that SIR2 is subject to degradation by the 26S proteasome (Dryden et al., 2003) and we observed increased levels of 26 protease regulatory subunit 7 in MTLE.

Taken together, mechanisms leading to cytoskeleton alterations may include oxidative stress, aberrant phosphorylation or impaired transcription/protein synthesis machinery. There are inevitable confounding factors including medication, the post-mortem vs *ex vivo* comparison, age differences, although no correlation of parameters with age were observed (Table 4). Medication administered to patients with MTLE was never reported to modulate cytoskeleton or the other significantly different proteins. 2-DE also does not allow to analyse all expression forms of individual proteins and therefore one obtains no information how representative a so-called ''isoform'' is for the overall levels of proteins. Cytoskeleton changes may represent or lead to development of MTLE.

Acknowledgement

This study was funded in part by a grant from Österreichische Nationalbank (grant number: 9195).

References

Baas PW (2002) Neuronal polarity: microtubules strike back. Nat Cell Biol 4: 194–195

Babb T, Brown WJ (1987) Pathological findings in epilepsy. In: Engel J Jr (ed) Surgical treatment of epilepsies. Raven Press, New York, pp 511–540

Bernert G, Fountoulakis M, Lubec G (2002) Manifold decreased protein levels of matrin 3, reduced motor protein HMP and hlark in fetal Down's syndrome brain. Proteomics 2: 1752–1757

Brady S, Colman DR, Brophy P (2003) Subcellular organization of the nervous system: organelles and their functions. In: Squire LR, Bloom FE, McConnell SK, Roberts JL, Spitzer NC, Zigmond MJ (eds) Fundamental neuroscience. Academic Press, San Diego, pp 79–114

Brown ME, Bridgman PC (2004) Myosin function in nervous and sensory systems. J Neurobiol 58: 118–130

Dos Remedios CG, Chhabra D, Kekic M, Dedova IV, Tsubakihara M, Berry DA, Nosworthy NJ (2003) Actin binding proteins: regulation of cytoskeletal microfilaments. Physiol Rev 83: 433–473

Dryden SC, Nahhas FA, Nowak JE, Goustin AS, Tainsky MA (2003) Role for human SIRT2 NAD-dependent deacetylase activity in control of mitotic exit in the cell cycle. Mol Cell Biol 23: 3173–3185

Dutcher SK (2001) The tubulin fraternity: alpha to eta. Curr Opin Cell Biol 13: 49–54

Eitzen G (2003) Actin remodeling to facilitate membrane fusion. Biochim Biophys Acta 1641: 175–181

Engel J Jr (1996) Introduction to temporal lobe epilepsy. Epilepsy Res 26: 141–150

Engidawork E, Gulesserian T, Fountoulakis M, Lubec G (2003) Aberrant protein expression in cerebral cortex of fetus with Down syndrome. Neuroscience 122: 145–154

Engidawork E, Lubec G (2003) Molecular changes in fetal Down syndrome brain. J Neurochem 84: 895–904

Fountoulakis M (2001) Proteomics: current technologies and applications in neurological disorders and toxicology. Amino Acids 21: 363–381

Fujii J, Ikeda Y (2002) Advances in our understanding of peroxiredoxin, a multifunctional, mammalian redox protein. Redox Rep 7: 123–130

Gulesserian T, Kim SH, Fountoulakis M, Lubec G (2002) Aberrant expression of centractin and capping proteins, integral constituents of the dynactin complex, in fetal down syndrome brain. Biochem Biophys Res Commun 291: 62–67

Hadfield JA, Ducki S, Hirst N, McGown AT (2003) Tubulin and microtubules as targets for anticancer drugs. Prog Cell Cycle Res 5: 309–325

Hendriksen H, Datson NA, Ghijsen WE, van Vliet EA, da Silva FH, Gorter JA, Vreugdenhil E (2001) Altered hippocampal gene expression prior to the onset of spontaneous seizures in the rat post-status epilepticus model. Eur J Neurosci 14: 1475–1484

Hoeffer CA, Sanyal S, Ramaswami M (2003) Acute induction of conserved synaptic signaling pathways in Drosophila melanogaster. J Neurosci 23: 6362–6372

Horne MM, Guadagno TM (2003) A requirement for MAP kinase in the assembly and maintenance of the mitotic spindle. J Cell Biol 161: 1021–1028

Jackson GD, Berkovic SF, Duncan JS, Connelly A (1993) Optimizing the diagnosis of hippocampal sclerosis using MR imaging. Am J Neuroradiol 14: 753–762

Kim SH, Fountoulakis M, Cairns NJ, Lubec G (2002a) Human brain nucleoside diphosphate kinase activity is decreased in Alzheimer's disease and Down syndrome. Biochem Biophys Res Commun 296: 970–975

Kim SH, Shim KS, Lubec G (2002b) Human brain nascent polypeptide-associated complex alpha subunit is decreased in patients with Alzheimer's disease and Down syndrome. J Investig Med 50: 293–301

Krapfenbauer K, Berger M, Lubec G, Fountoulakis M (2001) Changes in the brain protein levels following administration of kainic acid. Electrophoresis 22: 2086–2091

Krapfenbauer K, Engidawork E, Cairns N, Fountoulakis M, Lubec G (2003) Aberrant expression of peroxiredoxin subtypes in neurodegenerative disorders. Brain Res 967: 152–160

Krapfenbauer K, Yoo BC, Fountoulakis M, Mitrova E, Lubec G (2002) Expression patterns of antioxidant proteins in brains of patients with sporadic Creutzfeldt-Jacob disease. Electrophoresis 23: 2541–2547

Little E, Tocco G, Baudry M, Lee AS, Schreiber SS (1996) Induction of glucose-regulated protein (glucose-regulated protein 78/BiP and glucose-regulated protein 94) and heat shock protein 70 transcripts in the immature rat brain following status epilepticus. Neuroscience 75: 209–219

Lopez I, Ayala C, Honrubia V (2003) Synaptophysin immunohistochemistry during vestibular hair cell recovery after gentamicin treatment. Audiol Neurootol 8: 80–90

Lubec B, Weitzdoerfer R, Fountoulakis M (2001) Manifold reduction of moesin in fetal Down syndrome brain. Biochem Biophys Res Commun 286: 1191–1194

Lukasiuk K, Kontula L, Pitkanen A (2003) cDNA profiling of epileptogenesis in the rat brain. Eur J Neurosci 17: 271–279

Marangos PJ, Schmechel DE (1987) Neuron specific enolase, a clinically useful marker for neurons and neuroendocrine cells. Annu Rev Neurosci 10: 269–295

Mueller SG, Trabesinger AH, Boesiger P, Wieser HG (2001) Brain glutathione levels in patients with epilepsy measured by in vivo (1)H-MRS. Neurology 57: 1422–1427

Nadler JV (2003) The recurrent mossy fiber pathway of the epileptic brain. Neurochem Res 28: 1649–1658

North BJ, Marshall BL, Borra MT, Denu JM, Verdin E (2003) The human Sir2 ortholog, SIRT2, is an NAD^+-dependent tubulin deacetylase. Mol Cell 11: 437–444

Pollak D, Cairns N, Lubec G (2003) Cytoskeleton derangement in brain of patients with Down syndrome, Alzheimer's disease and Pick's disease. J Neural Transm Suppl 67: 139–148

Pollard H, Khrestchatisky M, Moreau J, Ben-Ari Y, Represa A (1994) Correlation between reactive sprouting and microtubule protein expression in epileptic hippocampus. Neuroscience 61: 773–787

Poskanzer KE, Marek KW, Sweeney ST, Davis GW (2003) Synaptotagmin I is necessary for compensatory synaptic vesicle endocytosis in vivo. Nature 426: 559–563

Reeves SA, Helman LJ, Allison A, Israel MA (1989) Molecular cloning and primary structure of human glial fibrillary acidic protein. Proc Natl Acad Sci USA 86: 5178–5182

Represa A, Pollard H, Moreau J, Ghilini G, Khrestchatisky M, Ben-Ari Y (1993) Mossy fiber sprouting in epileptic rats is associated with a transient increased expression of alpha-tubulin. Neurosci Lett 156: 149–152

Sato K, Abe K (2001) Increases in mRNA levels for Talpha1-tubulin in the rat kindling model of epilepsy. Brain Res 904: 157–160

Schuller E, Gulesserian T, Seidl R, Cairns N, Lubec G (2001) Brain t-complex polypeptide 1 (TCP-1) related to its natural substrate beta1 tubulin is decreased in Alzheimer's disease. Life Sci 69: 263–270

Shetty AK, Zaman V, Shetty GA (2003) Hippocampal neurotrophin levels in a kainate model of temporal lobe epilepsy: a lack of correlation between brain-derived neurotrophic factor content and progression of aberrant dentate mossy fiber sprouting. J Neurochem 87: 147–159

Shim KS, Lubec G (2002) Drebrin, a dendritic spine protein, is manifold decreased in brains of patients with Alzheimer's disease and Down syndrome. Neurosci Lett 324: 209–212

Suckau D, Resemann A, Schuerenberg M, Hufnagel P, Franzen J, Holle A (2003) A novel MALDI LIFT-TOF/TOF mass spectrometer for proteomics. Anal Bioanal Chem 376: 952–965

Sussman MA, Sakhi S, Tocco G, Najm I, Baudry M, Kedes L, Schreiber SS (1994) Neural tropomodulin: developmental expression and effect of seizure activity. Brain Res Dev Brain Res 80: 45–53

Takehashi M, Alioto T, Stedeford T, Persad AS, Banasik M, Masliah E, Tanaka S, Ueda K (2004) Septin 3 gene polymorphism in Alzheimer's disease. Gene Expr 11: 263–270

Tocco G, Bi X, Vician L, Lim IK, Herschman H, Baudry M (1996) Two synaptotagmin genes, Syt1 and Syt4, are differentially regulated in adult brain and during postnatal development following kainic acid-induced seizures. Brain Res Mol Brain Res 40: 229–239

Vlkolinsky R, Cairns N, Fountoulakis M, Lubec G (2001) Decreased brain levels of 2′,3′-cyclic nucleotide-3′-phosphodiesterase in Down syndrome and Alzheimer's disease. Neurobiol Aging 22: 547–553

Wang X, Phelan SA, Forsman-Semb K, Taylor EF, Petros C, Brown A, Lerner CP, Paigen B (2003) Mice with targeted mutation of peroxiredoxin 6 develop normally but are susceptible to oxidative stress. J Biol Chem 278: 25179–25190

Weitzdoerfer R, Fountoulakis M, Lubec G (2002) Reduction of actin-related protein complex 2/3 in fetal Down syndrome brain. Biochem Biophys Res Commun 293: 836–841

Yamamoto T, Toyoda C, Kobayashi M, Kondo E, Saito K, Osawa M (1997) Pial-glial barrier abnormalities in fetuses with Fukuyama congenital muscular dystrophy. Brain Dev 19: 35–42

Yang JW, Czech T, Lubec G (2004) Proteomic profiling of human hippocampus. Electrophoresis 25: 1169–1174

Yang JW, Rodrigo R, Felipo V, Lubec G (2005) Proteome analysis of primary neurons and astrocytes from rat cerebellum. J Proteome Res 4: 768–788

Yenari MA (2002) Heat shock proteins and neuroprotection. Adv Exp Med Biol 513: 281–299

Yoo BC, Kim SH, Cairns N, Fountoulakis M, Lubec G (2001a) Deranged expression of molecular chaperones in brains of patients with Alzheimer's disease. Biochem Biophys Res Commun 280: 249–258

Yoo BC, Vlkolinsky R, Engidawork E, Cairns N, Fountoulakis M, Lubec G (2001b) Differential expression of molecular chaperones in brain of patients with Down syndrome. Electrophoresis 22: 1233–1241

Zhu H, Zhu C, Hao J, Meng X, Wang L, Chen D (2000) Screening of novel epilepsy-related genes and isolation and identification of cDNAs. J Tongji Med Univ 20: 10–12

Authors' address: Prof. Dr. Gert Lubec, CChem, FRSC (UK), Department of Pediatrics, Medical University of Vienna, Waehringer Guertel 18, A-1090 Vienna, Austria,
Fax: +43-1-40 400 3194, E-mail: gert.lubec@meduniwien.ac.at